Investigation of annealing effects and film thickness dependence of polymer solar cells based on poly(3-hexylthiophene)

Gang Li, Vishal Shrotriya, Yan Yao, and Yang Yang

Additional information on J. Appl. Phys.

Investigation of annealing effects and film thickness dependence of polymer solar cells based on poly(3-hexylthiophene)

Gang Li, Vishal Shrotriya, Yan Yao, and Yang Yang[a)]
Department of Materials Science and Engineering, University of California—Los Angeles,
Los Angeles, California 90095

Regioregular poly(3-hexylthiophene) (RR-P3HT) is a promising candidate for polymer photovoltaic research due to its stability and absorption in the red region. In this manuscript, we report polymer photovoltaic devices based on RR-P3HT:methanofullerene [6,6]-phenyl-C_{61}-butyric acid methyl ester (PCBM) 1:1 weight-ratio blend. We studied the effects of annealing temperature and time on the device performance for devices annealed before and after cathode deposition. Thermal annealing shows significant improvement in the performance for both types of annealing conditions, with postproduction annealing being slightly better. For devices with a 43-nm-thick active layer, maximum power conversion efficiency (PCE) of 3.2% and fill factor up to 67% is achieved under Air Mass 1.5, 100-mW/cm^2 illumination. We performed atomic force microscopy and ultraviolet-visible absorption spectroscopy on the P3HT:PCBM films to explain the effect of thermal annealing. By keeping the optimized thermal annealing condition and by varying the active layer thickness, we fabricated devices with PCE up to 4.0%, which is the highest efficiency reported so far for this system. © *2005 American Institute of Physics.* [DOI: 10.1063/1.2008386]

I. INTRODUCTION

Photovoltaic (PV) cells have become more and more attractive as a truly clean, renewable energy source. The biggest obstacle of the crystalline silicon-based PV is the high semiconductor manufacturing cost. Polymer-based photovoltaic devices have shown promising potential as an alternative energy source.[1] In addition to low material and fabrication costs, polymer PV cells also provide properties such as mechanical flexibility and durability, and unlimited potential from advances in organic chemistry unachievable in inorganic semiconductor counterparts.[2] The efficiencies of polymer photovoltaic devices are mainly limited by the low carrier mobility[3] and short exciton diffusion lengths of polymers.[4] However, worldwide research on polymer photovoltaic cells in the last few years has resulted in significant improvement in the efficiencies of these devices[5–8] and has shown the possibility of putting them into practical applications.

Polymeric solar cells based on conjugated polymer/fullerene donor/acceptor (D/A) bulk-heterojunction blend system so far provide the main progress in improving photovoltaic cell efficiency.[6–9] Among these D/A systems, poly(3-hexylthiophene) (P3HT) and [6,6]-phenyl-C_{61}-butyric acid methyl ester (PCBM) blend is most promising.[10–12] This is primarily because of some unique properties of P3HT over other polymers, including high degree of crystallinity, high hole mobility in regioregular state (10^{-4} to 10^{-2} cm^2/V s), extended absorption in the red region (to 650 nm), and environmental stability. Padinger *et al.*[11] reported a power conversion efficiency (PCE) of 3.5% under Air Mass 1.5 (AM1.5) global illumination in P3HT/PCBM 1:2 weight-ratio blend system after thermal annealing and electrical con-

ditioning. Recent studies on P3HT/PCBM blend systems show that the absorption in the thin films is significantly quenched in the P3HT/PCBM 1:2 system compared to a 1:1 system, resulting in a much weaker red region absorption in the former.[13] Studies also showed that devices with 1:1 weight ratio show the highest power conversion efficiency.[13,14] However, no PCE over 3.5% has been reported for the "optimized" 1:1 weight-ratio system. In this paper, we extended our studies on photovoltaic cells with P3HT/PCBM 1:1 weight ratio. Thermal annealing condition was found very important for improving short circuit current, fill factor, and therefore the efficiency of the device. The optimized annealing conditions were further applied to devices with varying film thickness, resulting in PCE up to 4.0% [under Air Mass 1.5 global (AM1.5G) 100-mW/cm^2 illumination] for devices with ~63-nm active layer thickness.[15]

II. EXPERIMENT

The polymer photovoltaic cell in this study consists of a layer of P3HT/PCBM blend thin film sandwiched between transparent anode indium tin oxide (ITO) and metal cathode. P3HT acts as the *p*-type donor polymer and PCBM as the *n*-type acceptor in the active layer. Before device fabrication, the ITO- (~150 nm) coated glass substrates are first cleaned by ultrasonic treatment in detergent, de-ionized water, acetone, and isopropyl alcohol sequentially. This is followed by spin coating a thin layer (~30 nm) of poly(3,4-ethylenedioxythiopene) (PEDOT): poly(styrenesulfonate) (PSS) (Baytron P VP A1 4083) to modify the ITO surface. After baking at 120 °C for 1 h, the substrates are then transferred into a nitrogen-filled glove box (<0.1 ppm of O_2 and H_2O). To make a P3HT/PCBM 1:1 weight-ratio solution, P3HT is dissolved in 1,2-dichlorobenzene (DCB) to make a
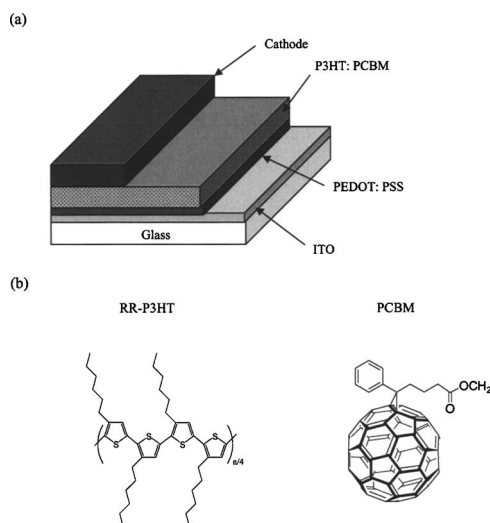
[a)]Electronic mail: yangy@ucla.edu

FIG. 1. (Color online) (a) Schematic of a typical device structure of polymer bulk-heterojunction photovoltaic device fabricated in this study and, (b) chemical structures of the constituent materials in the active layer.

FIG. 2. (Color online) UV-Vis absorption spectra obtained for P3HT:PCBM thin films (with PCBM concentration=50 wt %) before and after annealing at different temperatures. The annealing time here is 10 min for all the films.

17-mg/ml solution, followed by stirring the solution for ~12 h at 40 °C in the glove box. The P3HT/PCBM blend is spin coated onto the substrates and the thickness of the polymer films is controlled by changing the spin speeds. Finally the cathode, made of 25 nm of Ca and 100 nm of A1, is thermally evaporated in a deposition chamber in the glove box under a vacuum of ~10^{-6} Torr. The active area of the device, defined by shadow mask, is 0.11 cm^2. Either the films or the finished devices are annealed directly on top of a hotplate in the glove box, and the temperature is monitored by using a thermocouple touching the top of the substrates. After removal from the hotplate, the substrates are immediately put onto a metal plate at the room temperature. For obtaining absorption measurements, thin films of P3HT:PCBM blends are spun cast from the solution in DCB onto quartz substrates, and a Varian Cary 50 ultraviolet-visible (UV-Vis) spectrophotometer was used to obtain the spectra. A Digital Instruments Multimode Scanning Probe Microscope was used to obtain the atomic force microscopy (AFM) images from the films spun cast on glass substrates. The current-voltage (*I-V*) curves were measured with a Keithley 2400 source meter, under illumination from a ThermoOriel 150-W solar simulator with AM1.5G filters. A Newport 818T-10 thermopile detector is used to calibrate the light intensity. The thicknesses of the films were measured using a Dektak profilometer. All the devices were tested inside a N$_2$-filled glove box.

III. RESULTS AND DISCUSSION

Figure 1 shows the typical device structure of a polymer photovoltaic cell fabricated in this study and the chemical structures of the materials used. The details of device fabrication process and material and device characterization techniques are given in Sec. II. Figure 2 shows the effect of thermal annealing on the UV-Vis absorption spectra for the thin films of P3HT:PCBM (with PCBM concentration of 50 wt %) spun cast on quartz substrates. The absorption spectra show a considerable change after thermal annealing of the
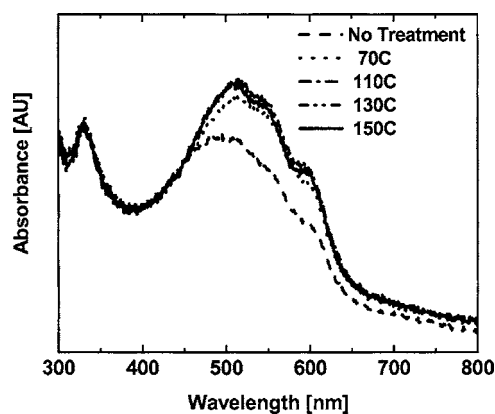
films. The films were annealed under an ambient of nitrogen inside the glovebox at atmospheric pressure. For the untreated film the peak absorption wavelength (λ_{max}) is 495 nm with a shoulder at ~594 nm and a barely visible shoulder at ~545 nm. The effect of thermal annealing on the absorption spectra is apparent even for the films treated at a temperature of 70 °C. After annealing at this temperature the λ_{max} is 509 nm showing a redshift, and the shoulders at 545 and 595 nm become more distinguishable. At 110 °C, the peak wavelength further redshifts to ~515 nm although the position of the two shoulders shows no change. Films treated at 130 °C show similar behavior. Further increasing the temperature to 150 °C, however, results in a blueshift of λ_{max} by about 8 to ~507 nm. After thermal annealing the peak at ~330 nm, which corresponds to PCBM, shows no change at any temperature. The annealing time for all the above temperatures was 10 min. We also measured absorption spectra for the films annealed at 70, 110, and 130 °C, for time periods ranging from 4 to 40 min, but only the spectra for 10 min of annealing are shown for the sake of simplicity. The other curves (not presented here) show a similar behavior. Since the thickness of all the films is similar (~80 nm), the change in the peak absorption wavelength during thermal annealing may be attributed to an increased interchain interaction among P3HT chains. The increased interchain interaction among the P3HT chains because of thermal annealing results in more delocalized conjugated π electrons, the lowering of the band gap between π and π^*, and the increase of the optical π-π^* transition which results in the observed redshift in the peak absorption wavelength.

The interface between the polymer and the electrode plays an important role in determining the electrical characteristics of the devices[16,17] and the morphology of the spun-cast polymer film has to be studied in order to understand the nature of the metal-polymer interface. In order to understand the morphological changes that occur in the polymer layer as a result of thermal annealing, we studied the AFM images of the active layer surface before and after annealing at different temperatures. Figure 3 shows the AFM images for samples that have undergone various thermal treatments. For the as-cast film (with no thermal treatment) the surface is very smooth with a rms roughness of 0.377 nm. However,
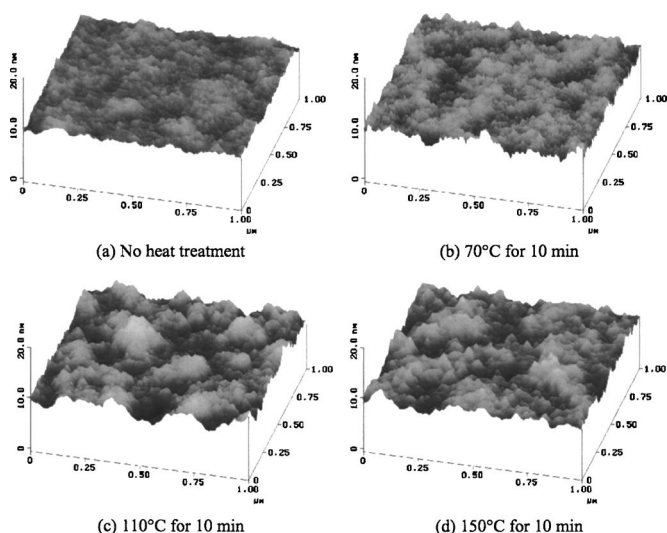
FIG. 3. (Color online) AFM height images of the surface of the active layer consisting of P3HT:PCBM (in 1:1 weight ratio) (a) before annealing, and after annealing at (b) 70 °C, (c) 110 °C, and (d) 150 °C. The annealing time for all the films was 10 min. The P3HT:PCBM films were spin coated on top of PEDOT:PSS-coated ITO glass.

after undergoing thermal treatment at 70, 110, and 150 °C for a period of 20 min each, the rms roughness becomes 0.662, 0.91, and 0.75 nm. The surface becomes rougher as the annealing temperature is increased to 70 and 110 °C, but on further increasing the temperature to 150 °C the surface becomes less rough compared to the film treated at 110 °C. Figure 3 also shows the change in the texture of the film after annealing at different temperatures. The film in Fig. 3(c) shows not only a higher roughness compared to the other films but also a much coarser texture with broad hill-like features compared to the other films. In the later part of this paper we will present the current-voltage characteristics for the photovoltaic devices where the active layer had undergone thermal treatment as described above. As we will show later, the best device performance and the highest efficiency are obtained for the devices with the active layer thermally treated at 110 °C. The obvious relation between the device performance and the surface roughness of the films, concluded from the morphology study, is that the higher roughness of the film will give higher efficiency device. One possible reason for this might be the increased contact area between the polymer film and the metal cathode for the films with higher surface roughness (i.e., for the films treated at 110 °C), which may result in a more efficient charge collection at the interface. It is known that the diffusion length of charge carriers in organic materials is often only a few nanometers,[4] and only those carriers generated near the electrodes will be collected and give rise to a photocurrent. Therefore the increased contact area will definitely have an effect on the efficiency of charge collection at the metal-polymer interface. The increased surface roughness might also enhance internal reflection and improve light collection, which would also increase device efficiency. We integrated the surface area of our roughest film and found that the surface area is only <0.1% more than that of a completely flat surface. This indicates that the above mentioned mechanisms
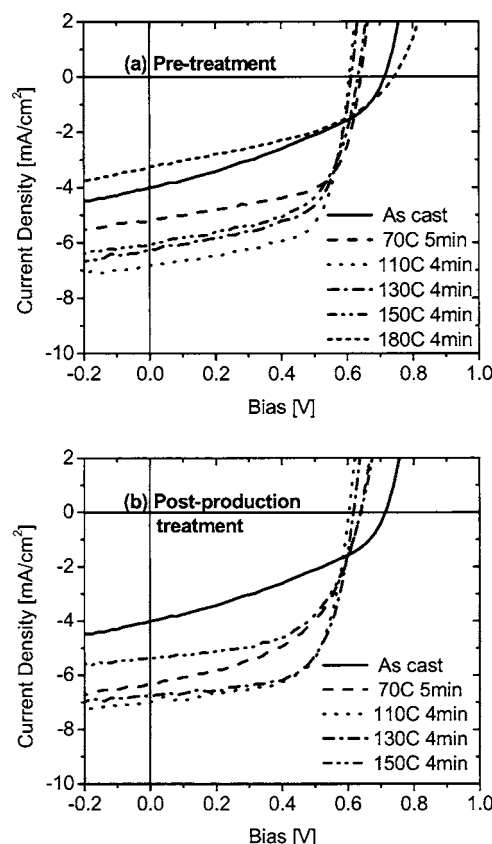

FIG. 4. (Color online) *I-V* characteristics under an illumination of 100 mW/cm^2 (AM1.5G) for devices that have undergone annealing (a) pretreatment and (b) postproduction treatment. The different curves represent different annealing temperatures ranging from RT to 180 °C.

only play a minor role in the device efficiency enhancement. Instead, the annealing enhances the ordered structure formation (as indicated by vibronic peaks in the absorption spectra). Higher absorption and an increase in the carrier mobility are most likely the reasons for the efficiency enhancement.

Figure 4 shows the *I-V* characteristics under illumination for photovoltaic devices that have undergone thermal annealing after spin coating the active layer but before cathode deposition (pretreatment) and for the devices that have undergone annealing after cathode deposition (postproduction treatment). The device performance depends heavily on the annealing conditions as clearly seen from the figure. For pretreatment conditions, the devices that are annealed at 110 °C show the best performance with efficiency as high as 2.8% ($t=20$ min), followed by the ones that are treated at 130 °C with efficiency ~2.3% ($t=20$ min). Further increasing the temperature to 150 and 180 °C results in performance degradation with highest efficiencies of 2.2% and 1.0%. From the AFM images (see Fig. 3), the annealing at 110 °C results in a rougher active layer surface than at other temperatures. The best performance of the devices for roughest polymer surface suggests a rougher metal-polymer interface is more suited for efficient charge collection. Higher roughness at the interface may also result in the presence of more defect sites that can increase exciton decomposition at the interface, thereby increasing the charge generation. For postproduction treatment conditions the devices that are treated at 110 °C show the
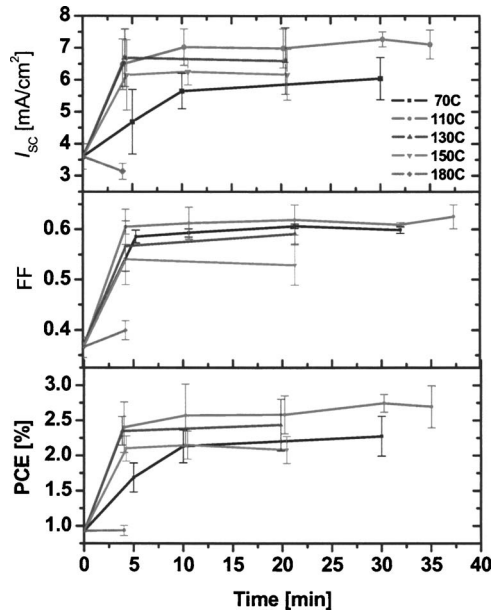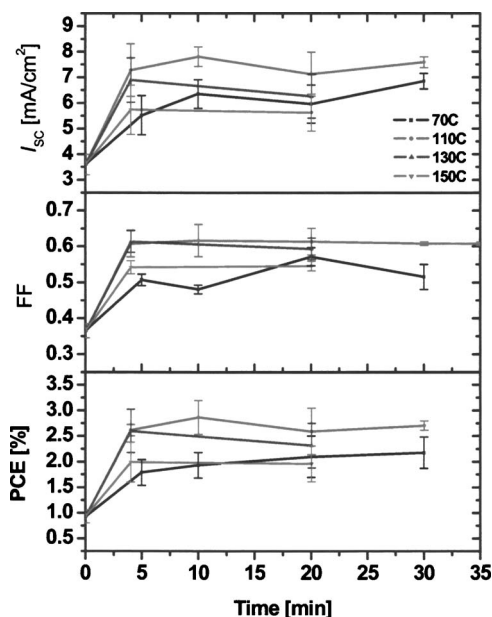
FIG. 5. (Color online) Short circuit current, fill factor, and power conversion efficiency plotted as a function of annealing temperature and time for pretreatment annealing.

TABLE I. Series resistance calculated from *I-V* plots in the dark for PV devices that have undergone heat treatment after spin coating the active layer (pretreatment) and after cathode deposition (post-treatment). The annealing time for all the devices here is 10 min.

Annealing temp. (°C)	Series resistance (Ω)	
	Pretreatment	*Post-treatment*
RT	50.8	50.8
70	49.8	30.4
110	30.1	21.3
130	30.3	26.0
150	26.1	26.7
180	18.8	

conditions, respectively. In both cases the measured values of I_{SC}, FF, and PCE show a drastic increase after thermal annealing. The effect is visible after annealing at even 70 °C and the highest values of the three parameters are obtained at 110 °C, with I_{SC}=7.6 mA/cm^2, FF=0.65, and PCE=3.0% for pretreatment, and I_{SC}=8.3 mA/cm^2, FF=0.67, and PCE=3.2% for postproduction treatment. We also measured the *I-V* characteristics of devices in the dark and calculated the series resistance from the log(I)-log(V) curves (Table I). The series resistance of the device R_S is given as the offset from linearity at high bias of the log current density versusvoltage plot.[18] The resistance of the device decreases on increasing the annealing temperature during pretreatment, which implies that the mobility of the charge carriers increases after annealing. The thermal treatment of P3HT films results in increased hole mobility.[19] Our measurement of series resistance supports these earlier findings, since an increase in the mobility will result in a lower resistance of the device. Based on the above electrical characterization, we found that the best annealing condition for PV cells based on an admixture of P3HT and PCBM in a 1:1 weightratio is at 110 °C for a 10-min postproduction. As a result of the optimization of the annealing conditions we consistently acheived device efficiency of more than 3.0%.

In a previous work, we have demonstrated that the thickness of the active layer plays an important role in determining the electrical characteristics of the device.[20] In order to further optimize the performance we fabricated devices with different active layer thickness. Keeping the optimized thermal annealing conditions (postproduction treatment at 110 °C for 10 min) as the same, we changed the active layer thickness of the photovoltaic devices and measured the *I-V* curves. *I-V* characteristics under an illumination of 100 mW/cm^2 (under AM 1.5G conditions) for the devices with varying active layer thickness are plotted in Fig. 7(a). The open-circuit voltage remains unchanged at about 0.60±0.02 V on changing the active layer thickness. However, the short circuit current density and the power conversion efficiency of the devices vary significantly with thickness as seen from Fig. 7(b). The I_{SC} varies from as low as 5.5 mA/cm^2 (for the device with active layer thickness, t=35 nm), to as high as 10.6 mA/cm^2 (for t=63 nm), and back to 6.5 mA/cm^2 (t=155 nm). The oscillatory behavior of I_{SC} as a function of thickness is similar to the effect we have

best performance with a highest efficiency of 3.2% (for t=10 min). The exact reason for better performance of the devices after postproduction treatment compared to pretreatment is unknown at this stage, but there is a possibility that the presence of a metal cap (in the form of the cathode) acts as a barrier during thermal annealing. The metallic layer might restrict the degree of vertical movement of the polymer chains and results in a better alignment of chains in the lateral direction. Figures 5 and 6 show the measured device operating parameters, namely short circuit current (I_{SC}), filling factor (FF), and PCE as a function of annealing temperature and time, for pretreatment and postproduction treatment

FIG. 6. (Color online) Short circuit current, fill factor, and power conversion efficiency plotted as a function of annealing temperature and time for postproduction treatment annealing.
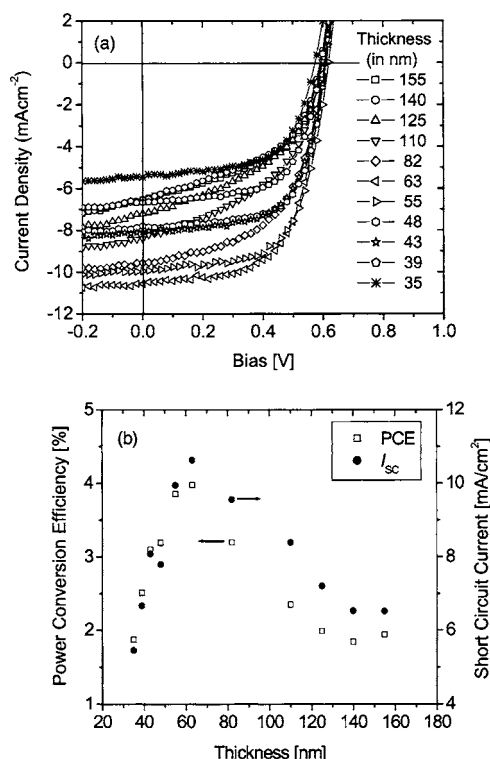
FIG. 7. (Color online) (a) *I-V* characteristics under illumination for photovoltaic device based on P3HT:PCBM (1:1 weight ratio) with different active layer thickness, and (b) short circuit current density and power conversion efficiency as a function of active layer thickness. All the devices here were annealed at 110 °C for 10 min of postproduction.

thickness. The results indicate that the device performance depends greatly on the polymer layer thickness. By comparing the efficiencies of devices with $t=140$ nm$(\eta=1.84\%)$ and $t=63$ nm$(\eta=4.0\%)$, we see that the efficiency can be increased by more than twice if an optimum thickness is achieved.

IV. CONCLUSION

In conclusion, we fabricated photovoltaic cells based on P3HT:PCBM by optimizing the annealing conditions and the active layer thickness. The best annealing condition for the device is postproduction treatment at 110 °C for 10 min. AFM images were used to study the polymer film morphology and the effect of surface roughness on charge collection efficiency at the metal/polymer interface. As a result, power conversion efficiency of the devices reached as high as 4.0% which is the highest efficiency reported so far for the polymer photovoltaic cells based on P3HT:PCBM system.

reported elsewhere for photovoltaic devices based on MEH-PPV:PCBM.[20] This oscillatory nature can be explained by modeling of carrier generation rate in the active layer near the anode/polymer and the cathode/polymer interfaces, as described in detail in Ref. 20. The optical effects play an important role in the variation of I_{SC} as a function of the active layer thickness. An efficiency of 4.0% is achieved for the device with $t=63$ nm. Table II shows the device parameters (PCE, V_{OC}, I_{SC}, and FF) as a function of active layer

TABLE II. Power conversion efficiency (PCE), open-circuit voltage (V_{OC}), short circuit current density (I_{SC}), and filling factor (FF) as a function of active layer thickness (t) for photovoltaic devices based on P3HT:PCBM with PCBM concentration equal to 50 wt %.

t(nm)	PCE (%)	V_{OC}(V)	I_{SC}(mA/cm^2)	FF
155	1.94	0.594	6.519	0.502
140	1.84	0.592	6.534	0.476
125	1.99	0.595	7.208	0.464
110	2.35	0.599	8.394	0.467
82	3.20	0.605	9.560	0.553
63	4.00	0.607	10.631	0.617
55	3.85	0.620	9.946	0.625
48	3.19	0.610	7.794	0.671
43	3.10	0.610	8.083	0.629
39	2.51	0.595	6.670	0.632
35	1.87	0.575	5.456	0.597

[1]*Organic Photovoltaics: Concepts and Realization*, C. J. Brabec, V. Dyakonov, J. Parisi, and N. S. Sariciftci (Springer, Heidelberg, 2003).
[2]C. J. Brabec, J. C. Hummelen, and N. S. Sariciftci, Adv. Funct. Mater. **11**, 15 (2001).
[3]P. W. M. Blom, M. J. M. de Jong, and M. G. van Munster, Phys. Rev. B **55**, R656 (1997).
[4]P. Peumans and S. R. Forrest, Appl. Phys. Lett. **79**, 126 (2001).
[5]N. S. Sariciftci, L. Smilowitz, A. J. Heeger, and F. Wudl, Science **258**, 1474 (1992).
[6]G. Yu, J. Gao, J. C. Hummelen, F. Wudl, and A. J. Heeger, Science **270**, 1789 (1995).
[7]G. Yu and A. J. Heeger, J. Appl. Phys. **78**, 4510 (1995).
[8]S. E. Shaheen, C. J. Brabec, N. S. Sariciftci, F. Padinger, T. Fromherz, and J. C. Hummelen, Appl. Phys. Lett. **78**, 841 (2001).
[9]F.-C. Chen, Q. Xu, and Y. Yang, Appl. Phys. Lett. **84**, 3181 (2004).
[10]N. Camaioni, G. Ridolfi, G. Casalbore-Miceli, G. Possamai, and M. Maggini, Adv. Mater. (Weinheim, Ger.) **14**, 1735 (2002).
[11]F. Padinger, R. S. Rittberger, and N. S. Sariciftci, Adv. Funct. Mater. **13**, 85 (2003).
[12]I. Riedel and V. Dyakonov, Phys. Status Solidi A **201**, 1332 (2004).
[13]V. Shrotriya, J. Ouyang, R. J. Tseng, G. Li, and Y. Yang, Chem. Phys. Lett. (in press).
[14]D. Chirvase, J. Parisi, J. C. Hummelen, and V. Dyakonov, Nanotechnology **15**, 1317 (2004).
[15]The efficiency value is not corrected for spectral mismatch. The mismatch factor for our measurement system is 0.8 as calibrated by National Renewable Energy Laboratory (NREL).
[16]J. Liu, Y. Shi, and Y. Yang, Adv. Funct. Mater. **11**, 420 (2001).
[17]H. Hoppe, M. Niggemann, C. Winder, J. Kraut, R. Hiesgen, A. Hinsch, D. Meissner, and N. S. Sariciftci, Adv. Funct. Mater. **14**, 1005 (2004).
[18]W. D. Jonston, Jr., *Solar Voltaic Cells* (Marcel Dekker, New York, 1980).
[19]A. Zen *et al.*, Adv. Funct. Mater. **14**, 757 (2004).
[20]V. Shrotriya, D. W. Sievers, F.-C. Chen, and Y. Yang (unpublished).